

# **Progress Report #2**

**TPF 5-387**

## **Development of an Integrated UAS Validation Center**

**Purdue University**

Prepared by  
Robert J. Connor  
Ayman Habibi  
John Mott

September 30, 2020

## **Project Background and Objectives**

Unmanned Aerial Systems (UAS) have the potential to drastically change how civil infrastructure is inspected, monitored, and managed. In the context of this document, a UAS is comprised of an Unmanned Aerial Vehicle (UAV), the scanning technology it carries, and the pilot. Deployment of UAS in areas such as bridge inspection and accident reconstruction will likely have far-reaching impacts and evolve over time, with new uses and users emerging as technology matures. With new technology, limitations exist until new protocols are established and industry must move forward with an appropriate level of caution. For example, speculation regarding the ability of a UAS to replace a human bridge inspector is frequently observed in trade magazines, presentations, and in the literature. With no standard tests to verify such claims, agencies are left to rely upon vendor's promotional material when making decisions about UAS deployment.

This pooled-fund study proposes to develop the standards, protocols, and testing requirements that a given UAS must meet and demonstrate for a particular application. As an example, considerations regarding UAS deployment for bridge inspection may include (but are not limited to) the following:

- Safety in constrained locations where line of site is limited
- Imaging system performance in poorly lit environments
- Control of the UAS while flying between large steel girders
- Adequate resolution of the imaging system for detecting the damage of interest

The objectives of the study are two-fold:

- Development of the specific criteria a given UAS must meet for each particular application.
- Determining how to validate that a given UAS meets the required criteria.
- The current industry is unregulated with regard to establishing the required level of performance for UAS in civil engineering applications. The results of this study will be the development of the performance measures and validation criteria that agencies can use when making decisions about deployment of UAS in the context of civil engineering.

This progress report presents detailed discussion regarding three primary topics:

- Proposed testing procedures developed to date as related to UAS.
- A discussion of important issues related to camera specifications and associated testing of such are also presented.
- Various factors the RT believes need to be considered by a UAS team prior to beginning a bridge inspection related to flight operations related to local turbulence adjacent to bridge structures.
- The following is a summary of progress as of September 30, 2020 related to TPF 5(387) "Development of an Integrated UAS Validation Center".

## Tests Under Development

### Obstacle Avoidance Test

#### General provisions and objective of the test

The purpose of this test is to assess the skills of the pilot of the UAV driving through a series of elements, called obstacles, that resemble real-life shapes and scenarios encountered while inspecting structures. The obstacles are going to be designed in different shapes and sizes complying with safe approaching distances for UAVs.

The obstacle course is designed to test the ability of the pilot to fly in a GPS-denied environment. Such places can be found underneath structures like bridges, or the GPS signal can be lost while flying close to the roof of structures. The pilot has to be trained to quickly change from preplanned flights or GPS-controlled flights to manual flights relying only on their skills, IMU (Inertial Measurement Unit) or barometric height. As a consequence, the obstacle course is also designed to test the characteristics of the vehicle to comply flight requirements determined by this test.

Additionally, defects are going to be presented in external and internal faces of the obstacles. To comply with this the test, the user will have to provide information related to those defects: type of defect, possible causes, requirement of further assessment. In the case of cracks or failures shown in faces of concrete and steel, dimensions for those failures will also be required.

#### Location of the obstacle course

In order to guarantee that the conditions of the test are equal every time that is applied, an enclosed space has been chosen. The obstacles have been adapted to fit a 40ft cargo container, presented in Figure 1.


Standard 40 Ft Cargo Container Specifications		
	Exterior Dimensions	40' L x 8' W x 8'6" H
	Interior Dimensions	39'5" L x 7'8" W x 7' 9 7/8" H
	Door Opening	7'8" W x 7'5" H
	Cubic Capacity	2,350 sq. ft.
	Tare Weight	8,000 lbs.
	Max Gross	67,200 lbs.
	Max Payload	59,200 lbs.

Figure 1 Cargo Container Specifications (Cargo Container HQ, 2019)

They are easy to find and purchase when necessary. Its enclosed characteristics allow to simulate a GPS-denied environment where the pilot will have to flight the UAV relying in its skills and the characteristics of the vehicle. In case of collision with any part of the obstacles or walls of the container, the test is terminated.

### GPS signal in indoor environment

GPS does not work in an indoor environment. Thus, UAS shall be capable of switching from GPS to manual or barometric height. Safe passage will be the result of combining IMU information and real-time observations of the obstacles to increase knowledge about true positions and avoid collision. The container will block the signal of most UAVs that will enter the test. Obstacles with roof in them will block any additional GPS signal, if such remains. In addition, at the far end of the obstacle course, the UAS will encounter NLOS (non-line-of-sight environment).

### Clearance Distance

In order to determine a safe clearance distance between obstacles, and a safe approaching distance between an UAV and obstacle, a literature review was carried to gather information on what it is currently used to inspect and monitor structures. Considering commonly used UAVs: DJI Matrice 100, DJI 5900, DJI Phantom 3 Pro, DJI Phantom 4, DJI Inspire 1, etc., an average clearance diameter was estimated to be 2.5 ft.

The concept of collision is also included. This means that every time inside the container, the UAV will have a collision cone of 2.5ft of diameter. The pilot can make the vehicle approach a distance closer to the recommended value, but it is not necessary in order to pass the test.

In addition, the concept of proximity effects is introduced. In other words: how close I can fly next to a structure before starting to lose control of the vehicle? In a closed space such as the container, wind will be controlled and reduced significantly to avoid interference; thus, no horizontal disturbance.

That is the reason why, in this environment only two proximity effects will govern: ground effect, and ceiling effect. Both of them are directly related to the diameter of the rotor, size of the UAV, payload, and clear distance between the UAV and the structure. Figure 2 illustrates these effects.



Figure 2 Ground effects (left) and Ceiling effects (right) in UAVs

The literature establishes different distances where these effects start to appear and take control of the vehicle. In general, a distance of 8 in was determined as the distance where proximity effects will start to govern.

Zones to consider when determining the dimensions of the obstacles

Summarizing previous findings, three zones have been determined in an UAV, depicted in Figure 3.

1. Zone delimited by the UAV (farthest part of the UAV)
2. Zone delimited by proximity effects only (where the UAV is close to collision and the pilot is losing control of the vehicle)
3. Zone delimited by proximity effects and pilot skills (UAV is pulled sideways and collision is imminent)

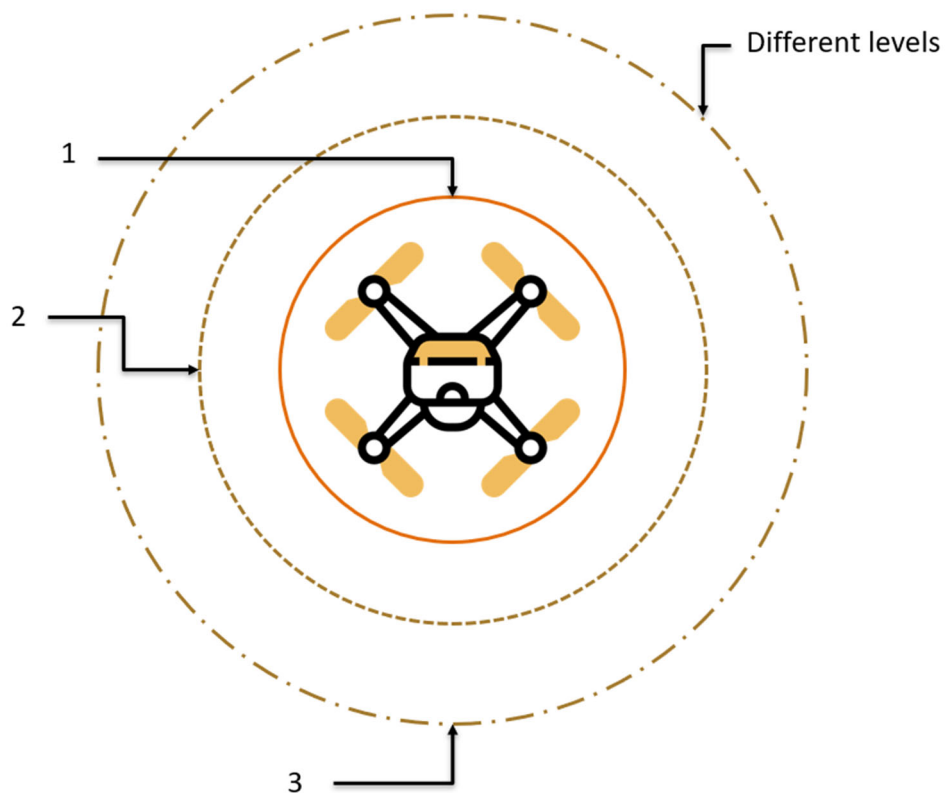


Figure 3 Zones surrounding an UAV

It is clear that it is crucial for this study to determine a standard value for number 2, which will be called the clearance distance. Several studies were performed close to tall structures, from

ground to roof, to determine where the pilot started to lose control over a typical UAV, and establish a general clearance distance, as presented in Figure 4.



*Figure 4 Trials to determine a safe clearance distance*

Several distances were determined based on these observations, but none of them was greater than the diameter of 2.5 ft already considered in the design. As a result, this is the distance that will govern the design.

## Mock Up

In determining the shape, size and quantity of the obstacles, several drafts were drawn considering a range variety of bridges, railroad ways, signal and luminaire structures. Issues with the design were encountered while performing a trial run in a mock up of the obstacle, by drawing its possible location inside a container. This first real application is presented in Figure 5. The issues were solved by changing the shape and order of three obstacles, rotating one obstacle, and adapting the clearance distance for obstacles 1, 2, and 3.



Figure 5 First trial of Obstacle Course

## Obstacle Course

After further analysis, seven obstacles were selected to fit inside the container and they are presented in Figure 6, next to their dimensions and clear distances. Figure 7 presents their heights, and Figure 8 is a 3D representation of the entire mock-up.

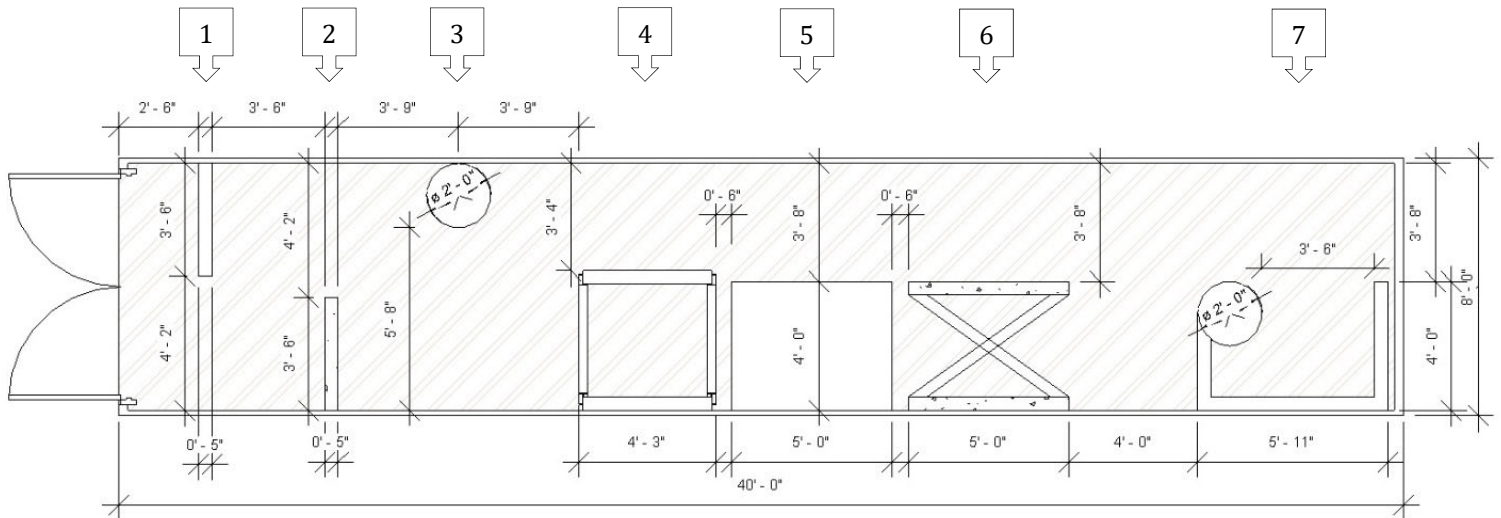


Figure 6 Plan view of the obstacle course

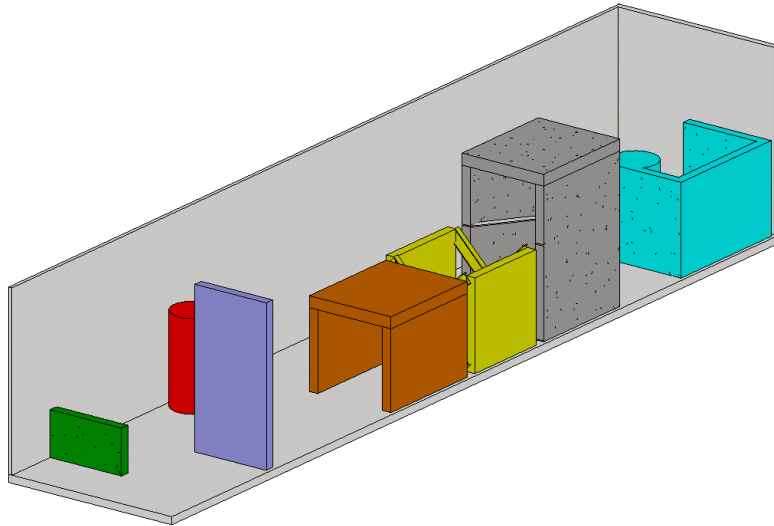
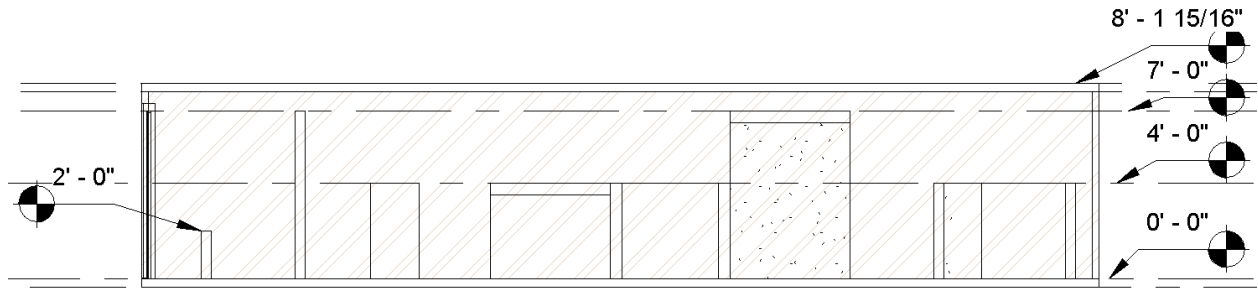
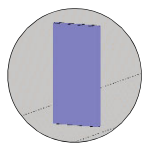
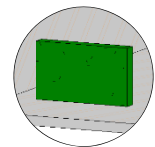


Figure 8 3D view of Obstacle Course

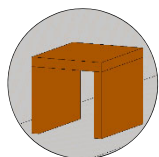
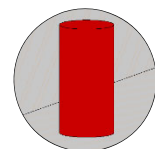
### Brief Description of Obstacles

**Obstacle 1:** rectangular faces where defects are going to be located. Main focus on spalling in concrete, delamination, and cracks. Represents small areas in structures.



**Obstacle 2:** rectangular faces. Main focus on cracks, delamination, and spalling. Possible inclusion of 3D printed elements in its faces. Obstacle representing most common type of geometries found in tall and slender structures or structural elements.

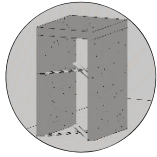
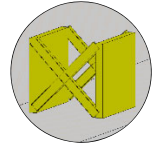
**Obstacle 3:** tube shape representing circular slender and tall structures, such as towers, signal, and luminaire structures. Also represents the shape of circular columns, and foundation piles.



**Obstacle 4:** represents a flight underneath structures with long spans. Main focus on defects on top and side faces. The UAV will not have GPS signal inside the container but this obstacle adds another block to that signal, if any remains.

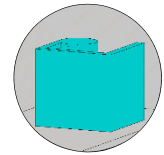


*Obstacle 5:* an obstacle that represents truss bridges and any steel element located in the side faces of its structure. Inspection shall focus on defects in the steel. The skills of the pilot are a key element navigating this obstacle.



*Obstacle 6:* focused on bridge elements, tall structures and skills of the pilot to fly between obstacles while focusing on the target to inspect. Points of interest on side elements, corrosion, connections, high altitude navigation

*Obstacle 7:* representing locations in structures where the pilot will not be able to closely follow the UAV, and in order to navigate in locations where Line of Sight is null, the pilot needs to rely most of the time in real-time images and video, and its skills to maneuver the UAV. Damages in internal faces will be placed.



## Defects

Two main concepts have been considered for defects inside the obstacle course: images of images, and 3D elements.

## Images of Images

Visual inspection is often applied by the inspector to detect possible failures in the structure and to suggest other measures that could range from further analysis with other non-destructive methods to immediate retrofitting or pause in the normal operations of the structure.



*Figure 9 Visual inspection of a bridge in S-BRITE*

When the inspector cannot approach the structure with his own eyes and hands, technology tools like UAVs are required. Needless to say, this technology would not replace a ‘face-to-face’ inspection, but it is an effective way to assess and suggest immediate actions. While using the

UAV to capture images and video of the desired structure in places the inspector cannot reach, they rely on those visual representations to carry the information to assess the status of the structure, such as the ones presented in Figure 9.

The idea behind the concept of 'images of images' is that in this test, the pilot will encounter defects in the obstacles represented by images from real defects in common structures. When they take a picture in the obstacle course, they will have the same conditions of light and wind any time and any place where the container is located, making the test under controlled-environment conditions.

An image of an image does not have the same quality as an image. But when the inspector analyzes an image taken from a structure, they do not take into account the number of pixels of the image, or its brightness or contour. What matters is if the defects are identifiable to the human eye, and if the inspector can provide feedback based on that information.

Under these circumstances, to prove that an image of an image is the same for an inspector than the original image, the concept of Just Noticeable Differences is introduced. In other words: how good is my image to the human eye that a regular person would not find notable differences between two images.

Two indices were implemented to prove that an image taken of a structure and the image of the same image of the structure will be the same at the eyes of an inspector, and as a result, will not affect its capability to detect what they would have been able to detect with the original image. These indices are: S-CIELAB and SSIM.

*The image quality metric S-CIELAB (CIE L\*a\*b\* Delta E metric) measures how exact the reproduction of a color is to the original when seen by a human observer. This process takes into account cone sensitivity of the eye, the ambient illumination, the spatial pattern of the targets, and other parameters important when the human brain is taken into account.*

*The SSIM (structural similarity index measure) provides a metric of the similarity of two images to the human eye. It considers image degradation and presents in its analysis luminance masking and contrast masking terms. It also takes into account the fact that the human brain most of the time would complete parts of an image, such as in blind spots. This phenomenon has been widely understood and recognized. Even if the image is not clear in certain spot, our brain would complete it based on the neighboring patterns. It will happen to an inspector seeing an original image and it will happen again seeing an image of an image.*

Images presented in Figures 10 and 11 were subjected to these concepts obtaining satisfactory results, proving that to the human eye, the images of images applied in this test will provide the same information to the inspector compared to the original image. Further analysis will focus on obtaining better parameters to caliber the models, and to apply the indices in images taken in other structures.



Figure 10 Image vs Image of an Image of bridge element in S-BRITE

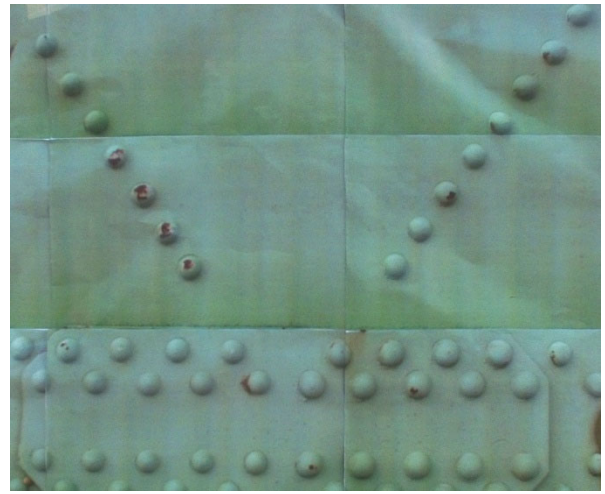
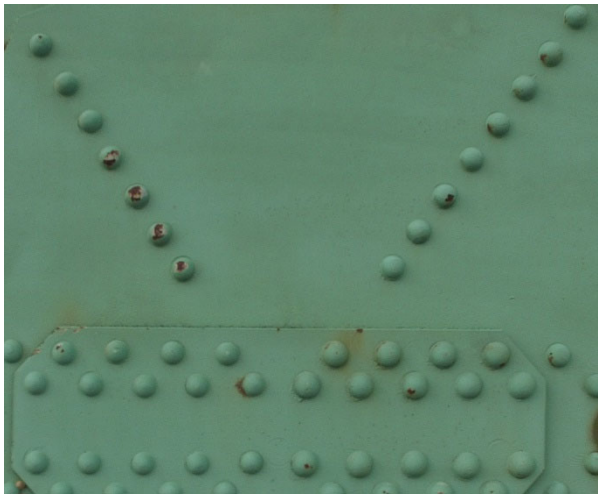
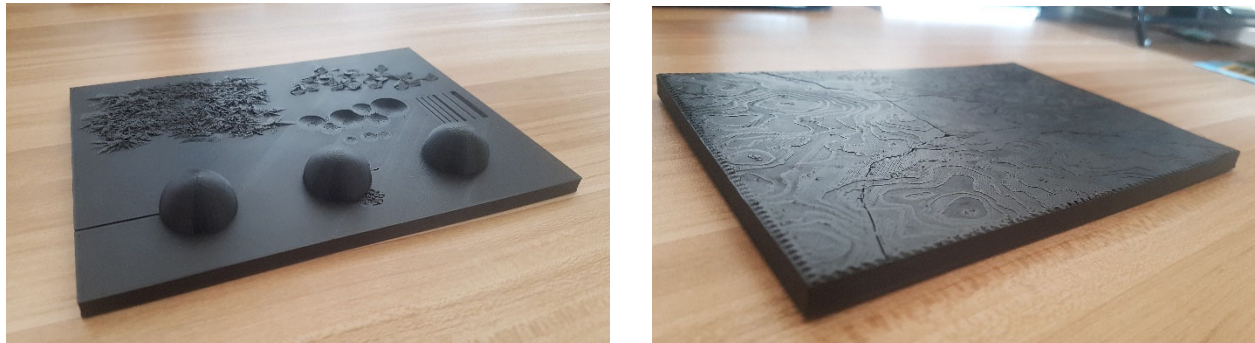


Figure 11 Image vs Image of an Image of bridge element in S-BRITE

## 3D printing

In an attempt to manipulate defects and present them with 3D components, models were developed to represent defects in concrete and steel: spalling, cracks with different sizes, delamination, blistering. Two models were designed and printed, presented in Figure 12.



*Figure 12 3D printed elements*

Images of these models have been obtained (Figure 13) and suggest changes to be implemented. New models will be developed to represent typical defects, another color of filament will be used and a paint will be applied to depict concrete characteristics.

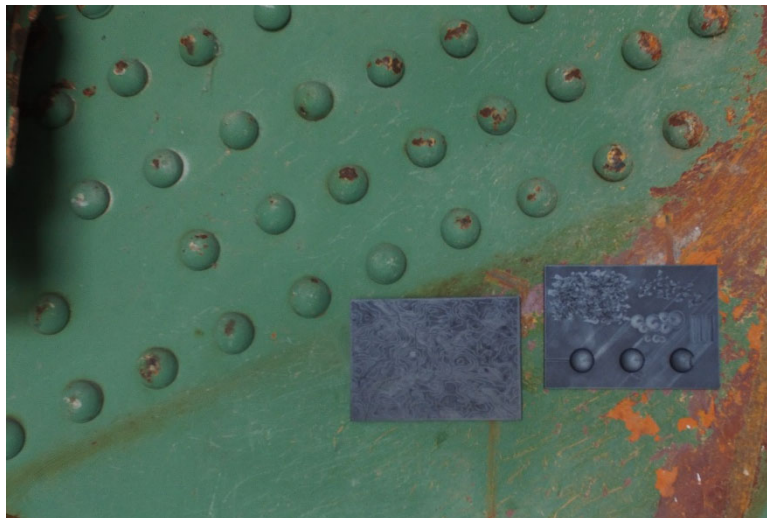


*Figure 13 3D printed elements in bridge structure*

## Wind Test

### Preliminary guidelines for a Wind Test

The objective is to test the ability of the UAS to provide desired data subjected to variable wind. Pre-planning of semi-autonomous GPS-controlled flight mission will be considered, thus allowing a matrix flight mission.

The same route will be followed at all times taking airborne photos of elements positioned in the test chamber. The path to be followed will ensure that UAS travels both with and against the wind. Following the test, an evaluation will be carried to assess if the photos and information collected is accurate and goes according to the specifications of this test. A preliminary draft is presented in Figure 14.

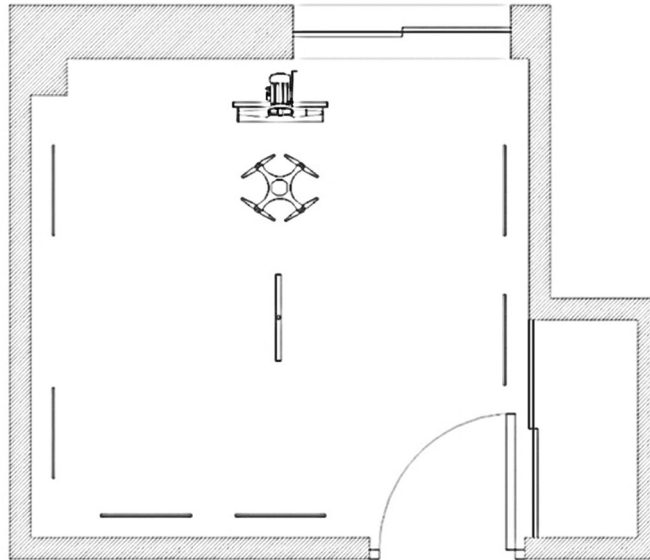


*Figure 14 Preliminary design for a Wind Test*

Proximity effects are going to be tested between:  $2R - 0.5 R$ , where  $R$  is the diameter of the vehicle, measured to its farthest edge. Tall and slender structures will be represented by elements inside the test. Lateral displacements combined with up-and-down movements will be required during the test.

## UAS Flight Protocol Testing

This section describes areas of research conducted for unmanned aerial system (UAS) inspection of bridge structures. Provided is a summary of the protocol required for UAS flight in a zero-grid airspace. Additionally, a summary of finalized simulation results for the identification of hazard zones created by wind surrounding bridge structures is provided.

### Zero-Grid Airspace UAS Flight

Zero-grid airspace is that airspace lying in close proximity to an airport and in which UAS flight is prohibited under FAR 107; such airspace is also referred to as a “no fly zone”. Through the use of a Certificate of Authorization (COA), however, allowable flight within a zero-grid airspace can be achieved. Coordination with local air traffic control (ATC) tower officials and online clearance resources are required for successful flight. Some UAS platforms may have alternate requirements for flight in zero-grid airspace. This research is conducted through the use of a DJI Phantom 3 Professional. With DJI UAS platforms specifically, No Fly Zone (NFZ) airspace flight is achieved through completing two steps:

1. Obtaining proper clearance using the FAA's LAANC system, and
2. Unlocking the UAS application through the DJI Flysafe website

Low Altitude Authorization and Notification Capability (LAANC) authorization can be requested through various mobile applications with which the FAA coordinates. The FAA suggests the use of “Kittyhawk”, a mobile app connected directly to FAA ATC personnel. Once proper LAANC clearance is provided by local ATC tower officials, a DJI unlock can be requested. This lock is placed on all UAS platforms located within restricted airspace regions, and can be removed with proper authorization through the “DJI Flysafe” website. The DJI Flysafe website requires an explanation of the flight clearance for the UAS to be unlocked, so a delay can result if FAA LAANC authorization has not yet been provided. Each of these steps requires an explanation of the flight parameters and justification of safety protocol. After both of these steps are complete, flight can continue as normal, as long as the appropriate safety protocols are followed.

A majority of test flights in this project consist of autonomous mapping of the bridge structures at S-BRITE research center. A “façade scan” function, or other vertical 3D imaging, allows the UAS to fly in a pattern tailored to the desired percentage of overlap, and capture images which can be used to create 3D models. Ideal bridge inspection can be done from point-cloud models created from 80% overlap imaging. These images are proposed to be used in conjunction with normal UAS bridge inspection once an appropriate system is developed and made more robust.

Some limitations exist with respect to infrastructure inspection flights apart from the time delays sometimes encountered with the authorization request process. One additional limitation is battery life, as it is common that detailed imaging of an entire bridge side can take more than 20 minutes. This is a typical value for battery life expectancy in UAS platforms. In previous flights, batteries have lasted this length of time; however, UAS are programmed to perform a return to home function and auto-land when battery levels reach 15%, sometimes restricting flight times.

This can be overcome with route coordination to pause and resume inspection during a battery change. At this point, the limitation devolves to the availability of charged batteries.

### Wind-Induced UAS Hazard Zones Surrounding Bridges

Figure 1 presents an integrated hazard model depicting regions where potential danger exists for UAS operation. Areas that are shaded red contain any of the following characteristics: a velocity gradient greater than 5 m/s per meter, fluid values indicating significant turbulence, or collision potential due to proximity to the bridge structure, combined with local aerodynamic effects. Areas shaded orange include any of the following traits: the UAS position can be altered considerably by local aerodynamic effects, a velocity gradient reaches a value between 2 and 5 m/s per meter, or fluid values indicate moderate turbulence.

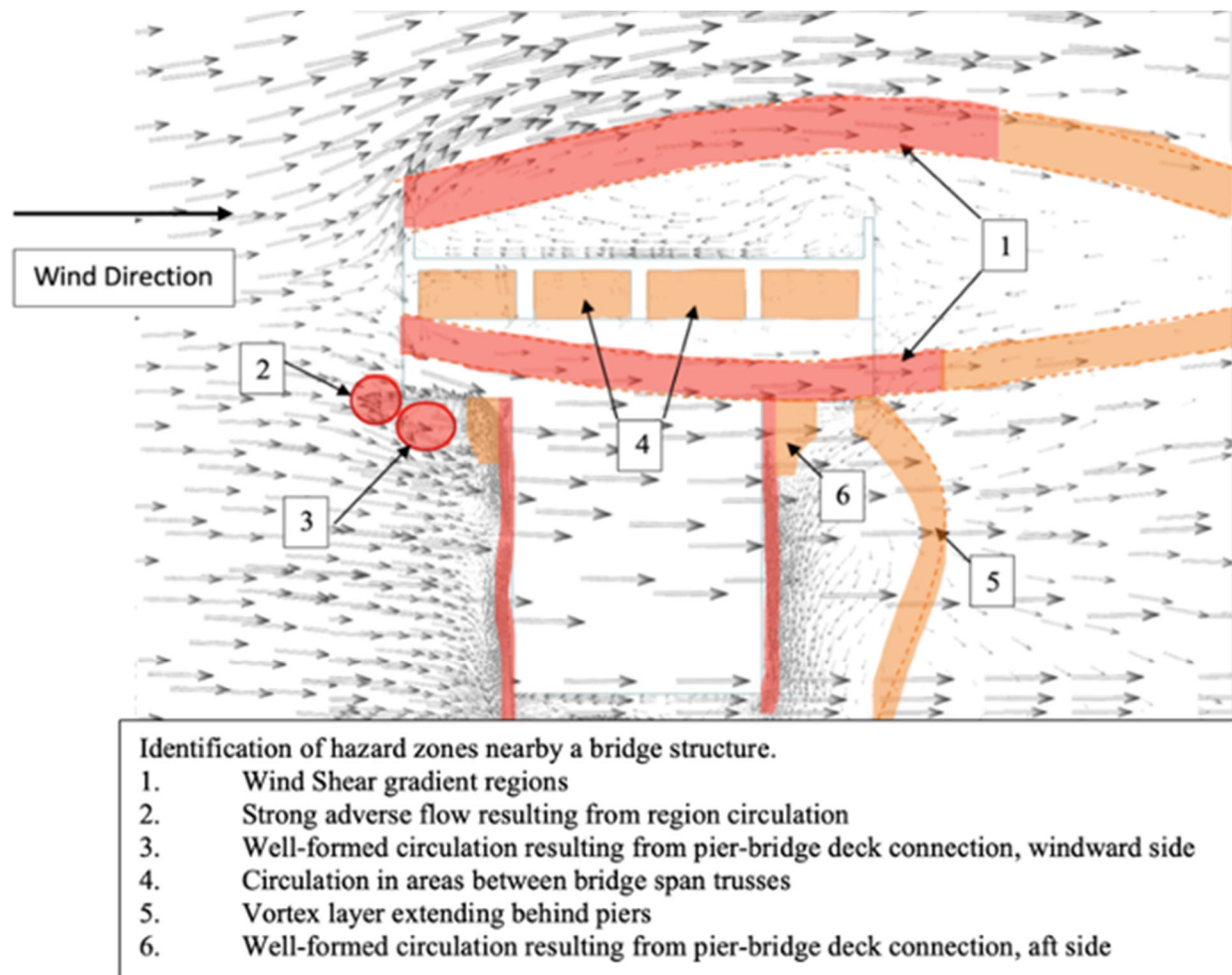


**Figure 15: Identification of Hazard Zones for 10 m/s Wind Velocity.**

One identifiable hazard resulting from airflow interactions with bridge structures is wind shear. Free stream flow extends beyond the bridge deck while lower pressure values beyond the bridge deck create a region of adverse flow. The length of this region depends on the free stream wind velocity, and the geometric shape of the bridge deck. Simulation points placed in this area can

show flow field characteristics that extend beyond the bridge deck. Table 4 shows results from simulations where wind velocity is varied.

**Table 4. Velocities within Aftward Wind-Shear Pocket.**

Point distance from bridge deck (m)	Average Wind Velocity (Z-direction) (m/s)			
	2 m/s	5 m/s	10 m/s	15 m/s
0.5	-0.13	0.24	-0.33	-1.16
2	-0.11	0.31	-0.38	-1.14
4	-0.09	0.23	-0.92	-1.42
6	0.63	2.56	3.21	5.85
8	0.72	3.78	3.88	7.06
12	1.12	4.23	7.85	13.84

The results indicate that the adverse flow pocket is different for changing values in initial wind velocity. A 4-meter adverse flow region of -1 m/s is seen for initial 15 m/s initial wind velocity. The structure of this pocket is similar at a 10 m/s freestream wind velocity; however, streamline reattachment occurs sooner, indicating lower local velocities. At wind speeds below 10 m/s, turbulent flow is present; however, the adverse flow pocket is not as well defined. At wind velocities between 5 and 10 m/s, wind can still be a potential hazard in areas surrounding the bridge deck. An effective moment can be created on a UAS when flying in this region. This moment can considerably jeopardize the stability of the aircraft, possibly leading to loss of UAS control.

Considerable circulation and turbulence also exist in front of and behind bridge piers. Increased turbulent kinetic energy (TKE) and specific dissipation rate (SDR) values indicate greater turbulence within these regions. Circulation develops at a substantial level with just 5 m/s of initial wind velocity; subsequently a one-meter region of circulation appears where the bridge deck and pier connect. Air circulation unpredictability suggests 5 m/s wind velocities would make this area a non-optimal zone for controlled UAS flight. Even at wind speeds between 5 and 10 m/s, force vectors in these areas can grow large enough to place operating UAS at risk for permanent control loss. Further analysis not provided here offers greater detail of these findings, as well as mathematical and theoretical information necessary for research replicability.



## UAS Flight in GPS-Denied Environments

The development of a UAS test course has presented some challenges when flying indoors; more specifically, within structures made of steel, concrete, or steel-reinforced concrete. There are several UAS functions that “require” the availability of a stable GPS signal. These operations are as follows:

- Position hold (fixed-space hover)
- Return to home
- Autonomous flight/pre-planned flight/path following
- Object/area avoidance

These operations use GPS for the mapping of surroundings and location sequencing, and the comparison of this information with information from inertial sensors is necessary for overall controlled flight. Return to home functioning can be eliminated by the denial of a GPS signal, causing the UAS to be “stuck” in space if no other mitigating systems are on board. The pilot is then responsible for guiding the UAS to safety or employing other methods to complete the UAS flight. The GPS signal also is responsible for the fixed-space position hold functioning. GPS is used to determine state variables that hold the UAS steady and feed the inertial sensors with directions for steady flight. The state variables that hold a UAS in steady, level, fixed flight (position, velocity, acceleration, attitude angles, and attitude rates) are determined when the GPS coordinates and surrounding characteristics are relayed to the inertial sensors, which keep the UAS in a fixed position. The inertial sensors are typically composed of three gyroscopes which measure 3D angular rates, and three accelerometers which measure the 3D acceleration. Without GPS, the UAS is able to hold its position, but does not have an absolute reference and is prone to drift over time.

It is common that without a GPS signal the inertial sensors are still capable of holding the UAS in a fixed position with respect to its environment. Still, the UAS is prone to state variable drift as a result of the inertial tools overcompensating during the time integration. To mitigate this, several neural network-based systems have been designed by other researchers to map the surroundings of the UAS, helping it to make decisions for which it is usually reliant on a GPS signal. In one example of such methodology, onboard LIDAR scanners are used to sense the physical surroundings using LIDAR pulses, timing them to determine how long they take to return to the sensor. The inertial sensors record the craft’s movements and are assisted by an onboard camera for visual tracking.

Even with the limits placed on a UAS in a GPS-denied environment, flight is still possible. With a live video feed, a pilot is able to manually fly a UAS through enclosed spaces. The risk of crash and UAS loss is increased; however, with appropriate training and planning, flight is still possible. Operational risks must be considered; for example, the loss of video feed and line of sight would render a pilot unable to see the UAS to safely operate it. Additionally, more technology is being developed to make GPS-denied flight possible. NASA is sponsoring several entities that are currently testing and developing a system that will map the surroundings of the GPS locally, and use that information for inertial sensor communication in-flight.

## Development of Objective Camera/Imaging Requirements

As a follow-up of prior work on evaluating the “Ground Sampling Distance - GSD” of an imaging system and the impact of the level of detail that can be discerned in the captured imagery, focus has been on the following tasks:

- a) Acquisition and testing of a mission planning package that can conduct UAV flights covering infrastructure elements (UgCS - <https://www.ugcs.com/>), and
- b) Development of a 2D/3D visualization tool to evaluate the ability of identifying artifacts in inspected elements.

### a) **UgCS Mission Planning**

The key advantage of UgCS is having the option of conducting a “Façade scan” (Fig. 1). This capability allows for the design of a vertical flight path by setting the minimum and maximum height, forward overlap and side overlap, as well as the distance to the façade. Using such parameters, UgCS can design the flight path automatically. In addition to this mode, UgCS can also support corner mapping of an object – i.e., multi-facades option is possible while keeping a constant distance from the mapped Façades at that corner (Fig. 2). UgCS also enables the control of the camera during the flight. As shown in Fig. 3-a, we can adjust the camera attitude by specifying the roll, tilt and yaw angles. As for camera triggering, UgCS can trigger camera automatically through a user-defined overlap, time interval – Fig. 3-b, or distance interval – Fig. 3-c. The team has conducted different missions for the acquisition of image blocks to test the capability of UgCS to collect imagery for 2D and 3D inspection/visilauzation as will be discussed next.

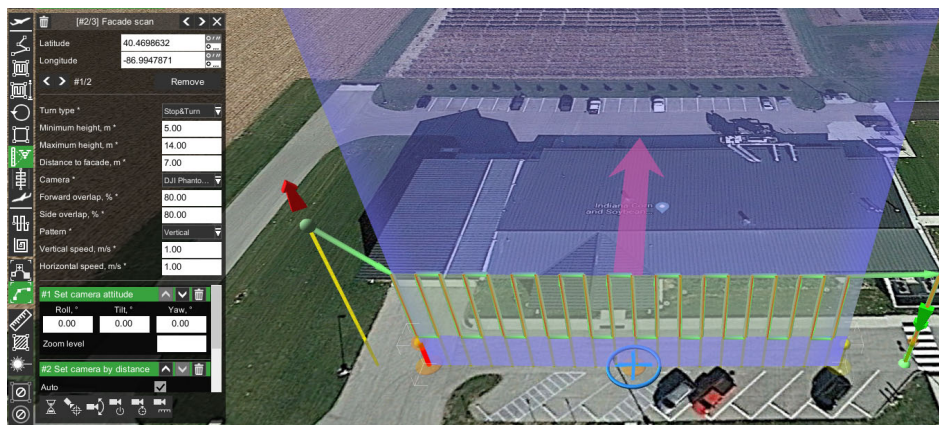


Fig.1 Façade scan mode (single façade)

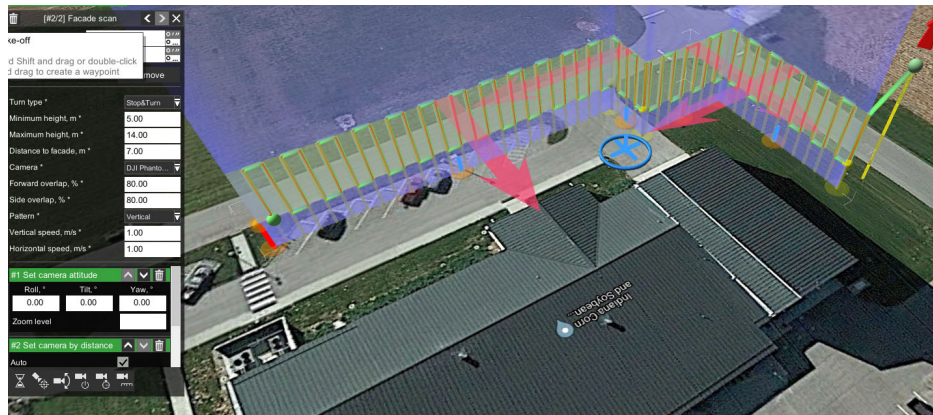


Fig.2 Façade scan mode (multi-facade)

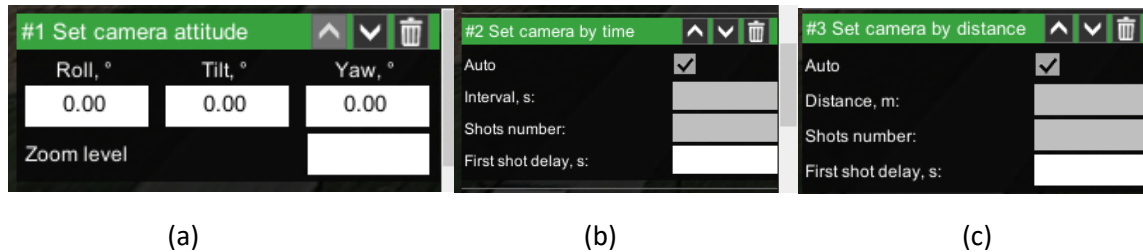
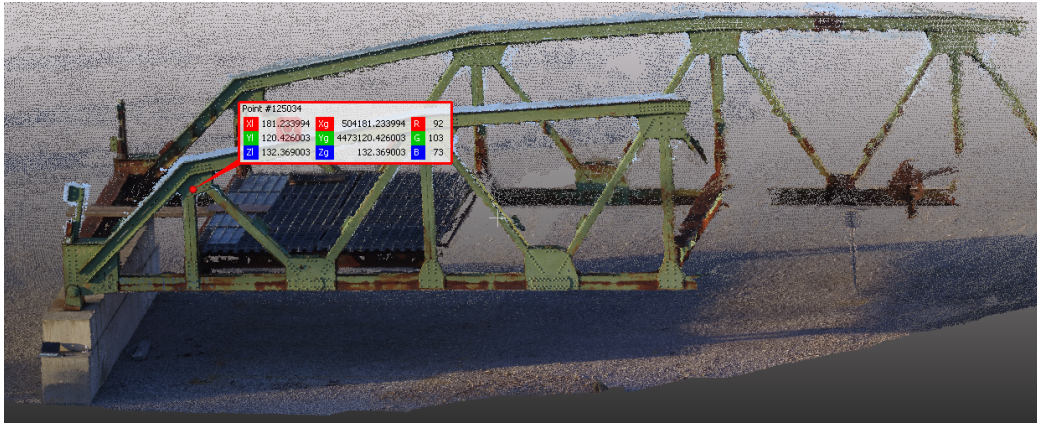


Fig.3 Camera settings: (a)attitude, (b)trigger by time, and (c) trigger by distance

### Image/Point Cloud Visualization

GSD is a numerical measure of the smallest detail that can be discerned in acquired imagery as a result of the pixel size and principal distance of the used camera as well as the camera-to-object distance. Beside such factors, there are other aspects, whose impact cannot be quantified, that could affect the ability of identifying details, such as aberrations, lighting condition, diffraction, and motion blur. To provide the overall capability of artifact identification, the team has developed an interactive visualization environment utilizing both the original 2D images and derived 3D point cloud through a Structure from Motion (SfM) triangulation process. Pix4d is an example of a commercially available SfM procedure for deriving 3D information from overlapping 2D images (<https://www.pix4d.com/>). The interactive visualization environment uses the Pix4D outcome from the triangulation of the collected images through UgCS. The 3D point cloud as well as the 2D images can be visualized as shown in Fig. 4 – 3D point cloud in Fig. 4-a and 2D images in Fig. 4-b. More specifically, the user can select a point in the 3D viewer window – Fig. 4-a. Then, the tool identifies all the images where this particular point is visible. Among these images, the image that is closest to the 3D point will be displayed in the image viewer window – Fig. 4-b. In addition, the tool will show a table with all the images where the selected object point is visible together of the distance between the camera and that point – Fig. 4-c. Any image in that table can be selected and the 2D image viewer window will refresh showing this image. Therefore, we can identify the impact of camera-to-object distance, lighting condition, and viewing angle on the level of detail that could be discerned. This environment together with the UgCS will be used to

capture and visualize imagery/point clouds under different lighting conditions/distances/viewing angles on discernable artifacts of controlled samples.



(a)



(b)

Visible Images		
	Camera 1	Distance: Camera
1	0	5.57993
2	1	5.40426
3	2	5.15433
4	3	5.0929
5	4	5.18583
6	5	5.34329
7	6	5.40934
8	7	5.19261
9	8	5.40301
10	9	5.3668
11	10	5.06109
12	11	4.80377

(c)

Fig. 4 Illustration of the 2D/3D visualization tool: (a) selected 3D point in the point cloud, (b) corresponding point in a visible image is shown, and (c) all images where the 3D point is visible are listed with together with the camera-to-object distance.